



HAL
open science

A modified well index to account for shear-thinning behaviour in foam EOR simulation

Antoine Soulat, Frédéric Douarche, Eric Flauraud

► **To cite this version:**

Antoine Soulat, Frédéric Douarche, Eric Flauraud. A modified well index to account for shear-thinning behaviour in foam EOR simulation. *Journal of Petroleum Science and Engineering*, 2020, 191, pp.107146. 10.1016/j.petrol.2020.107146 . hal-02551338

HAL Id: hal-02551338

<https://ifp.hal.science/hal-02551338>

Submitted on 22 Apr 2020

HAL is a multi-disciplinary open access archive for the deposit and dissemination of scientific research documents, whether they are published or not. The documents may come from teaching and research institutions in France or abroad, or from public or private research centers.

L'archive ouverte pluridisciplinaire **HAL**, est destinée au dépôt et à la diffusion de documents scientifiques de niveau recherche, publiés ou non, émanant des établissements d'enseignement et de recherche français ou étrangers, des laboratoires publics ou privés.

A modified well index to account for shear-thinning behaviour in foam EOR simulation

A. Soulat^{a,*}, F. Douarche^a and E. Flauraud^b

^aIFP Energies nouvelles, Geosciences Division, 1 et 4, avenue de Bois-Préau – 92852 Rueil-Malmaison Cedex – France

^bIFP Energies nouvelles, Applied Mathematics Division, 1 et 4, avenue de Bois-Préau – 92852 Rueil-Malmaison Cedex – France

ARTICLE INFO

Keywords:

Multiphase flow

Porous media

Foam

Shear-thinning

Injectivity

Well index upscaling

ABSTRACT

An accurate evaluation of injectivity is essential to the economics of any chemical EOR process. Most commercial simulators enable non-Newtonian behaviour modelling but it is often overlooked due to inadequate grid resolution. Indeed, in cases where shear-thinning fluids are injected in a reservoir, shear rates and viscosities in the vicinity of the wellbore can be poorly estimated if the spatial resolution of the well grid-blocks is too coarse. This results in biases in injectivity and economics which we discuss here in the context of foam-based displacements.

We first demonstrate that a poor evaluation of near-wellbore velocity leads to erroneously degraded injectivity on coarser grids when compared to a sufficiently refined reference grid. In order to correct these errors we propose new formulations of the well index that capture shear-thinning behaviour that the conventional Peaceman calculation fails to address. This modified well index is applied and validated in various scenarios of foam displacement simulation with radial grids. Our proposed solution, used under a simplified form as direct input in reservoir simulation, significantly enhances injectivity estimates without resorting to grid refinements or modifying the shear-thinning model of the injected foam. In most cases it yields results that are closer to those obtained using grid refinements than the Peaceman formula at a much more attractive computational cost. Additional work remains to complete our understanding of injectivity in more complex settings, especially when effects such as foam dry-out and destruction in the presence of oil are as important on sweep efficiency as its shear-thinning behaviour.

Our workflow successfully corrects biases in the estimation of injectivity and yields more accurate results and avoids resorting to time-consuming methods such as grid refinements and physical input data alteration. Moreover it is simple to implement in most commercial simulators and does not require using empirical criteria. However, it bears some limitations which we also discuss.

1. Introduction

Although they may prove very efficient, enhanced oil recovery (EOR) processes involving gas injection (such as steam and/or solvent injection) usually have poor sweep efficiency because of petrophysical heterogeneities, density contrasts and viscous instability between the displacing gas and the displaced fluids [20]. Injecting foam is a possible way to address this issue [35, 32].

Maintaining injectivity is key to the economics of any EOR processes, especially processes consisting of injecting a very low-mobility fluid. Indeed, injection rates often have to be reduced in order to keep the injection well pressure below fracture pressure; this is a recurrent topic in polymer or foam EOR [17, 41]. There are examples of disturbed field applications of chemical EOR due to unexpected fracturing during injection [18, 27, 36]. Moreover managing high foam injection rates is important in overcoming the segregation of the injected gas due to gravity [33].

However, predicting foam injectivity accurately in reservoir simulation implies the adequate capture of the non-Newtonian nature of foam [15, 10, 4, 5, 19]. Indeed, as illustrated in Fig. 1, the shear-thinning behaviour of foam leads

to a very large decrease of its apparent viscosity in the near-wellbore area, where flow velocities are usually substantial, thus enhancing its injectivity. It is worth mentioning that experimental data characterizing this behaviour in porous media is versatile and that this impacts the calibration of models and therefore their accuracy.

Most standard reservoir engineering workflows and commercial reservoir simulators [34, 9, 16] use the Peaceman equation [28] which fails to capture this effect as it assumes Newtonian behaviour. Attempts at upscaling shear-thinning effects in chemical EOR processes have been made before, often under formats not easily implemented in reservoir simulators and without predictive capability in the case of foam. The issue of adequately capturing shear-thinning behaviour has been addressed mostly in the case of polymer injection: Sharma et al. [37] for example proposed an empirical method that adjusts the parameters of the Peaceman equation to account for non-Newtonian mobility in the near-wellbore region. More recently, Li et al. [22] described a semi-analytical injectivity model implemented in UTCHEM, and Li et al. [23] generalized this model for the calculation of an apparent skin factor that may be used as a direct input parameter in any reservoir simulator. Leefink et al. [21] and Gong et al. [14] developed analytical models to estimate foam injectivity and proved that conventional models underestimate it; however their models are not practical for users of standard commercial simulators.

*Corresponding author

✉ antoine.soulat@ifpen.fr (A. Soulat); frederic.douarche@ifpen.fr (F. Douarche); eric.flauraud@ifpen.fr (E. Flauraud)

www.ifpenergiesnouvelles.fr (A. Soulat)

ORCID(s): 0000-0001-5943-6405 (F. Douarche)

A modified well index to account for shear-thinning behaviour in foam EOR simulation

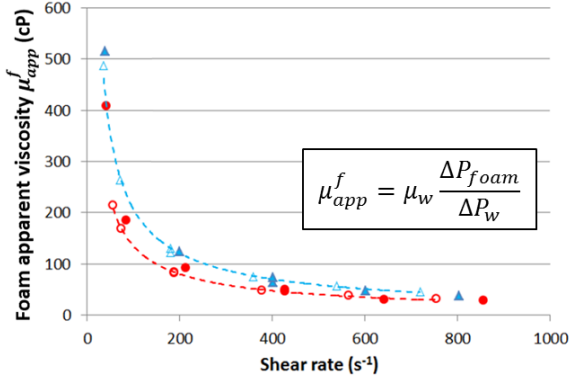


Figure 1: Coreflood measurements of foam apparent viscosity vs shear rate, showcasing the shear-thinning behaviour of foam (adapted from [5], which also compares the alteration of rock wettability (blue: original wettability; red: altered wettability); symbols denotes the presence (filled) or absence (empty) of oil).

In this paper, we first study the impact of gridding on the estimation of near-wellbore velocity and foam injectivity and show that insufficient spatial resolution leads to inaccurate rendering of pressures at the injector. Therefore we propose a well index model that enables shear-thinning behaviour to be accounted for. This modified well index is first expressed in a complex, full form that is at a later stage simplified to facilitate its use as direct input for reservoir simulation. This simplified form is validated with a one-dimensional radial reservoir model, then with two-dimensional Cartesian models, in two-phases systems (water and gas) as well as three-phases systems (water, gas and oil) involving an aqueous foaming agent component denoted surfactant.

2. Foam rheology in reservoir simulation

Two sorts of representations are usually distinguished when modelling foam flow in porous media: local equilibrium models and population balance models. Examples of reviews and comparisons of the different equations governing these models may be found in Ma et al. [26], Lotfollahi et al. [24] or Gassara et al. [11]. In this work we focus on semi-empirical models, which are a type of local equilibrium models, as they are implemented in most commercial reservoir simulation softwares such as EclipseTM, CMG StarsTM or PumaFlowTM.

In this study PumaFlowTM (exhaustively described in Braconnier et al. [7] and Gassara et al. [12]) was used to run simulations; in this simulator for example the gas mobility (which is the ratio of gas relative permeability over gas viscosity $\lambda_g = k_{rg}/\mu_g$) is multiplied by a mobility reduction factor FM when foam is present:

$$\lambda_g^f = FM \cdot \lambda_g \quad (1)$$

FM is a multi-parameter interpolation function that includes the contributions of physical parameters impacting the gas

mobility reduction and is defined as:

$$FM = \frac{1}{1 + (M_{ref} - 1) \prod_{i=1}^4 \mathcal{F}_i} \quad (2)$$

where M_{ref} is the maximum gas mobility reduction when the rock-fluid-additive system under consideration is at its optimal conditions and the \mathcal{F}_i functions describe the effect of surfactant concentration, water saturation, oil saturation, and gas velocity on foam viscosity.

The \mathcal{F}_1 function accounts for foam lamellas stability as a function of the local surfactant concentration in the water phase denoted C_w^s [38, 13], and is formulated as a normalized power law of C_w^s :

$$\mathcal{F}_1(C_w^s) = \left(\frac{\min(C_w^s, C_{w,ref}^s)}{C_{w,ref}^s} \right)^{e_s} \quad (3)$$

up to the minimum surfactant concentration threshold $C_{w,ref}^s$ at which foam may exist, where e_s is a modelling parameter. \mathcal{F}_1 function will be given ad-hoc values to account for surfactant concentration variations in the well gridblock, as reported in Table 1. The \mathcal{F}_2 and \mathcal{F}_3 functions account for the dry-out and oil saturation effects on foam stability which are not treated in this work (hence $\mathcal{F}_2 = \mathcal{F}_3 = 1$). Surfactant is assumed not to adsorb on the rock. Furthermore, physical phenomena such as foam instability during injection, pressure and temperature dependency of foam rheology and the impact of surfactant properties are not addressed in this work.

In semi-empirical models, foam can behave as a shear-thinning non-Newtonian fluid. In this work, we focus on the shear-thinning function \mathcal{F}_4 defined as:

$$\mathcal{F}_4(N_{cg}) = \left(\frac{N_{cg}^{ref}}{\max(N_{cg}, N_{cg}^{ref})} \right)^{e_c} \quad (4)$$

where N_{cg}^{ref} and e_c are model parameters and N_{cg} is the gas capillary number, which is defined as the ratio of the gas viscous forces over the capillary forces between gas and water in the presence of foam:

$$N_{cg} = \frac{\mu_g u_g^f}{\Phi \sigma_{wg}} \quad (5)$$

where u_g^f is the Darcy velocity of the foaming gas phase, Φ the porous medium porosity and σ_{wg} the interfacial tension between the water and gas phases. Other authors define the capillary number using either the total flow velocity instead of the gas velocity [25, 6, 42] or the gas interstitial velocity $v_g^f = u_g^f / (\Phi S_g)$ deduced from u_g^f [12]. Although differences in the formulation of the capillary number formulation may yield different results, overall the physics it conveys are the same.

A modified well index to account for shear-thinning behaviour in foam EOR simulation

Parameter	Value
Rock compressibility	10^{-5} bar $^{-1}$
Porosity Φ	0.08 (fraction)
Permeability k	30 mD
Water viscosity μ_w	0.37 cP
Water density ρ_w	1 g/cm 3
Gas viscosity μ_g	0.013 cP
Gas density ρ_g	0.987×10^{-3} g/cm 3
Water-gas interfacial tension σ_{wg}	10^{-2} N/m
Initial reservoir pressure	180 bar
Interval thickness h	25 m
Foam mobility reduction M_{ref}	22,000
Injected surfactant concentration	2 g/L
Injected foam quality f_g	0.8
\mathcal{F}_1 parameter e_s	1
\mathcal{F}_1 parameter $C_{w,ref}^s$	0.5 g/L
\mathcal{F}_4 parameter e_c	0.5
\mathcal{F}_4 parameter N_{cg}^{ref}	10^{-12}

Table 1
Reservoir and rock-fluid system properties and foam parameters.

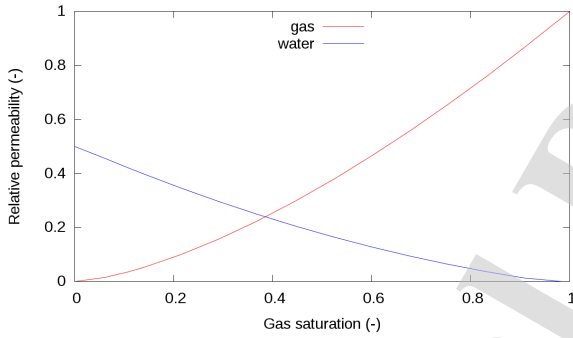


Figure 2: Relative permeability curves used in the two-phase system.

3. Errors in injectivity when applying the Peaceman equation

To start with, we consider a two-phase radial system where foam is injected continuously. A homogeneous and isotropic reservoir is modelled, with the injection well on rate constraint. Gas is injected at a volumetric flow rate of $Q_g = 120$ m 3 /day and water is co-injected at $Q_w = 30$ m 3 /day (all considered rates are taken at reservoir conditions). Foam quality f_g , which is the ratio of the volumetric flux of foamed gas over the total volumetric flux of gas and liquid, is therefore set to 0.8 at the well bottom. The details of the reservoir properties, rock-fluid system and foam model parameters are given in Table 1. Relative permeability curves are modelled using power laws and are reproduced in Fig. 2. The fluid system is modelled using a black oil model that is compositional in the water phase due to the foaming agent being transported by the water phase.

All effects on foam stability apart from gas velocity and

Gridblock radius r_0 (m)	Peaceman well index (cP · m 3 /day/bar)
2	16.10
10	9.79
20	8.37
30	7.72
50	7.03
75	6.57
100	6.27

Table 2
Well index values obtained using the Peaceman formula for the considered gridblock radii.

surfactant concentration are neglected. The variations of the foam model functions \mathcal{F}_1 , \mathcal{F}_4 and FM relative to the distance to the well are illustrated in Fig. 3.

The grids considered in this section were built with different block sizes resolutions Δr in the radial coordinate r . A high resolution model (sketched in Fig. 4) with a well gridblock radius r_0 of 10 cm, is surrounded by four intertwined cylindrical coronas of decreasing spatial resolutions such that $\Delta r_1 = r_0 = r_w = 10$ cm over 200 m, $\Delta r_2 = 1$ m over 2 km, $\Delta r_3 = 10$ m over 20 km and $\Delta r_4 = 100$ m over 100 km, eventually. This model has been validated as a reference where foam injectivity is accurately captured, since it is free of any arbitrary velocity cut-off due to coarse gridding in the near-wellbore area. It is worth noting that since the well gridblock radius r_0 coincides with the well radius r_w , the well index has been set to an arbitrarily large value in order to obtain a gridblock pressure that converges towards the well bottom hole pressure.

Using coarser grids, as sketched in Fig. 4, simulations were run with the standard Peaceman formula; the corresponding well index values are listed in Table 2. At first we consider continuous foam injection in a water saturated porous medium. We compare the bottom hole pressure obtained with the reference grid and the coarse grids. Results are displayed in Fig. 5. As expected the conventional Peaceman formula for injectivity overestimates the bottom hole pressure, and the discrepancy with the reference result increases with the size of the well gridblock: a gridblock radius of 50 m for example overestimates the bottom hole pressure by 72 bar, and a 100 m gridblock radius by 105 bar. The variation of this discrepancy with the well gridblock size is shown in Fig. 6. It can be noted that for gridblock radii close to the reference case (e.g. 2 m) the results obtained with the Peaceman formula are acceptable; however for well gridblock sizes usually employed in reservoir simulation it grossly underestimates injectivity.

Fig. 7 shows the change with time of the \mathcal{F}_1 and \mathcal{F}_4 functions in the well gridblock. The results obtained with coarse grids show a large difference with the reference grid, showing that velocity in the vicinity of the wellbore is underestimated; thus the shear-thinning behaviour of foam is overlooked and foam is exaggeratedly strong as indicated by the values reached by FM . The coarser the grid, the greater

A modified well index to account for shear-thinning behaviour in foam EOR simulation

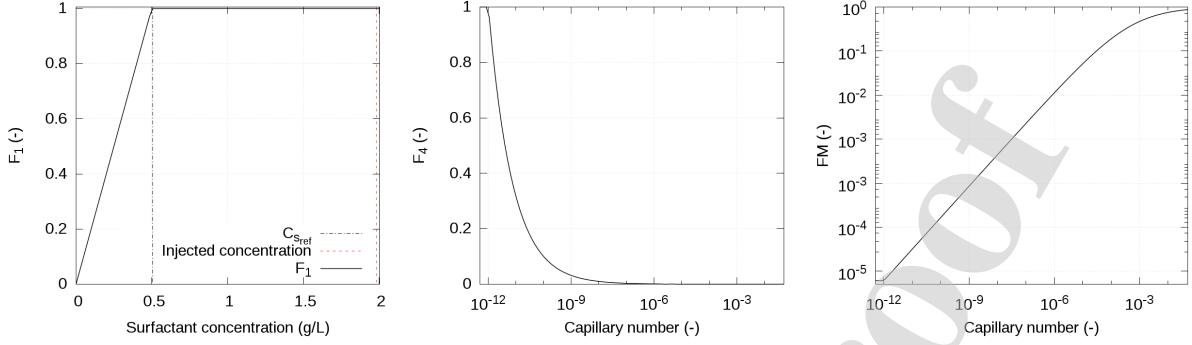


Figure 3: Variation of the \mathcal{F}_1 function relative to surfactant concentration in water and of the \mathcal{F}_4 and FM (assuming $\mathcal{F}_1 = 1$) functions relative to the capillary number.

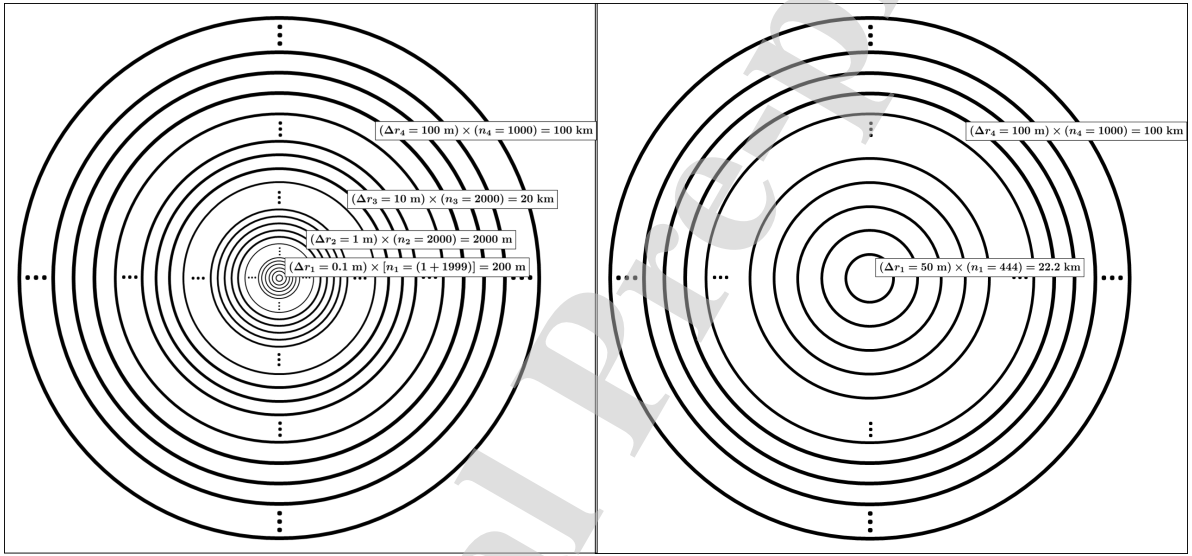


Figure 4: Sketch diagram representing the reference, fine resolution radial grid (left) as well as a coarse grid with a well gridblock radius of 50 m (right). The cell radial dimension Δr_i is increased tenfold every 2,000 cells with the well gridblock having a radius of 10 cm.

181 the error: the value of FM for a gridblock radius of 50 m is
 182 16 times smaller than the value obtained with the reference
 183 grid.

184 Moreover, there is also an effect of surfactant concentra-
 185 tion changes on bottom hole pressure: steady-state is reached
 186 later as the gridblock radius increases. This impacts the val-
 187 ues reached by the \mathcal{F}_1 function in the well gridblock since
 188 the injected solution dilutes quickly in coarser grids: it takes
 189 more than 80 days to reach a surfactant concentration greater
 190 than $C_{w,ref}^s$ in a 50 m radius well gridblock, while it is reached
 191 almost immediately in the reference case. The effect is pro-
 192 gressively eliminated as more surfactant is injected.

193 This effect of gridding on foam strength also affects satu-
 194 ration changes over time: the gas saturation values obtained
 195 at steady-state strongly differ from the reference grid as dis-
 196 played in Fig. 8. As expected this strongly impacts gas rela-
 197 tive permeability and total mobilities at the wellbore. This

198 can be explained since FM intervenes directly in the calcula-
 199 tion of gas relative permeability: an error in the estimation
 200 of FM yields an error in total mobility.

201 This demonstrates a coupling between saturation effects
 202 due to the two-phase nature of the system and velocity ef-
 203 fects, both impacted by gridblock size, which complicates
 204 the analysis of results; as a consequence, we will focus in
 205 this study on steady-state results.

206 4. Modified well index derivation

207 4.1. Peaceman well index calculation for 208 Newtonian fluids

209 Assuming radial flow, integrating Darcy's law over a ho-
 210 mogeneous and isotropic porous medium from the well ra-

A modified well index to account for shear-thinning behaviour in foam EOR simulation

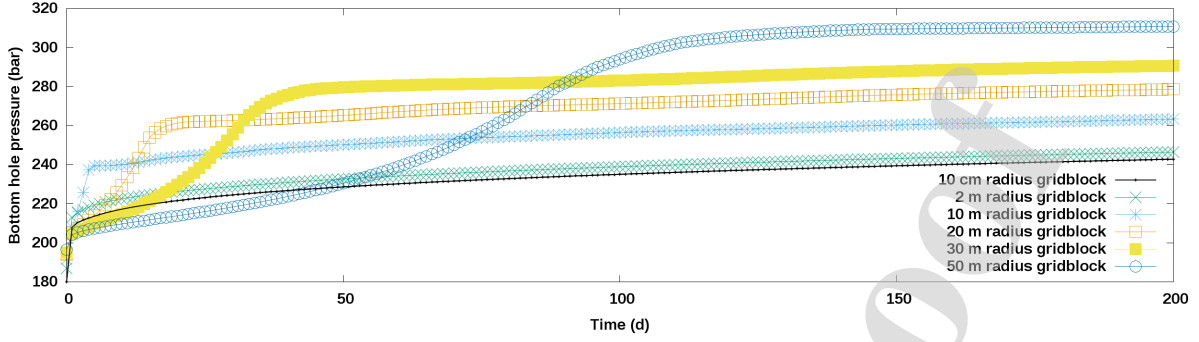


Figure 5: Radial model – injector bottom hole pressure vs time for various gridblock sizes.

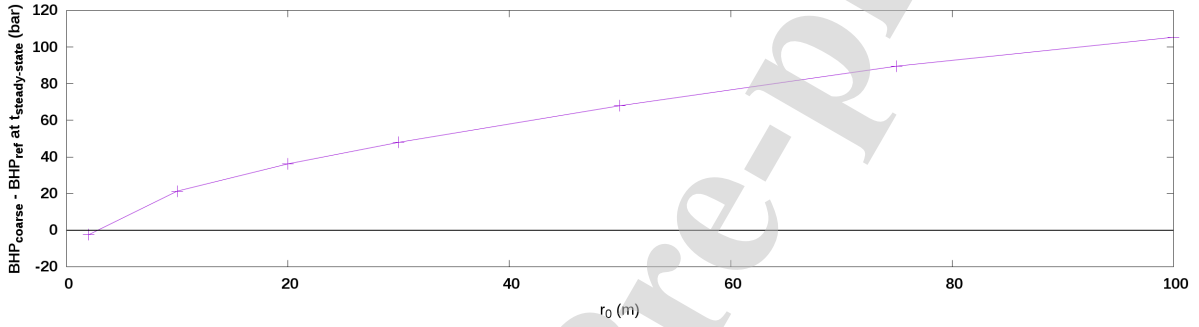


Figure 6: Radial model – injector bottom hole pressure at steady-state vs gridblock size.

211 dius r_w to a given radial distance r gives at steady-state:

$$P(r) = P_f + \frac{\mu Q}{2\pi h k} \ln\left(\frac{r}{r_w}\right) \quad (6)$$

212 where μ is the viscosity of the injected fluid, Q the injection
213 flow rate, h the thickness of the perforated interval, k
214 the porous medium permeability and P_f the flowing bottom
215 hole pressure. In order to compute the pressure in the well
216 gridblock, Peaceman [28] writes:

$$P(r) = P_0 + \frac{\mu Q}{2\pi h k} \ln\left(\frac{r}{r'_0}\right) \quad (7)$$

217 where P_0 is the pressure assigned to the well gridblock and
218 r'_0 the so-called equivalent radius. As shown by Peaceman
219 [28], in its simplest (5-point) formulation r'_0 can be found by
220 summing the steady-state fluxes between the well gridblock
221 and its four x - y neighbours; using the isotropy of the porous
222 media yields:

$$r'_0 = e^{-\frac{\pi}{2}} \Delta x_0 \approx 0.208 \Delta x_0 \quad (8)$$

223 where Δx_0 is the lateral dimension of the well gridblock in
224 a square Cartesian grid (where all gridblocks have the same
225 dimensions, i.e. $\Delta x_0 = \Delta x$). For a given well or perforation
226 Peaceman's well index, denoted WI_0 , is defined as:

$$Q = \frac{2\pi h k}{\mu \ln\left(\frac{r'_0}{r_w}\right)} (P_0 - P_f) \equiv \frac{WI_0}{\mu} (P_0 - P_f) \quad (9)$$

227 where skin has been omitted the sake of conciseness. Such
228 a result is obviously grid- and numerical-scheme-dependent
229 (for instance, in the case of a 9-point x - y scheme one no
230 longer has $r'_0 = e^{-\frac{\pi}{2}} \Delta x_0$). Furthermore, the above deriva-
231 tion also exists for anisotropic permeabilities as demonstrated
232 in [29].

233 Interestingly, other authors such as van Poolen and co-
234 workers have shown [31], prior to Peaceman, that the well
235 gridblock pressure P_0 can be derived by averaging the ex-
236 act single-phase pressure $P(r)$ over the well gridblock for
237 a steady-state isotropic radial flow [31, 30, 8]. While there
238 is little difference in the so-derived equivalent radius r'_0 ex-
239 pression as discussed in Peaceman [28] and the well index
240 definition remains the same, this approach provides a fer-
241 tile framework to average foam apparent viscosity over the
242 near-wellbore area according to the fluids velocity profiles
243 in an upscaling perspective. We propose such an approach
244 in the next section to derive a well index in the context of
245 two-phase shear-thinning foam steady-state flow.

4.2. Introduction of phase mobility

246 There are many ways to relate flow rate and pressure for
247 an injector well. In the case of foam injection where gas and
248 surfactant bearing water are co-injected, with both Q_g and
249 Q_w being injection constraints, Darcy's law written at the
250

A modified well index to account for shear-thinning behaviour in foam EOR simulation

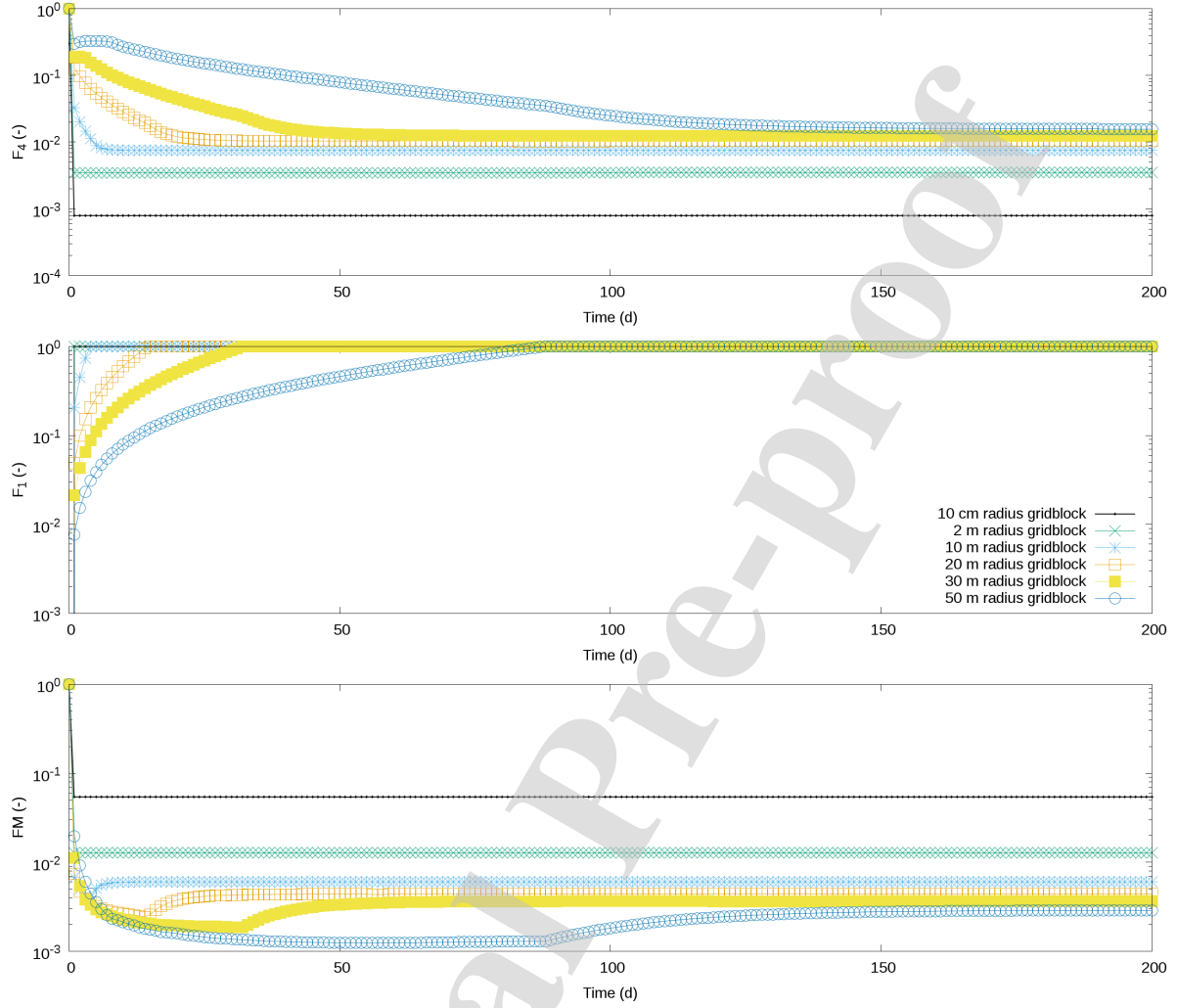


Figure 7: Radial model – \mathcal{F}_4 , \mathcal{F}_1 and FM functions values in well gridblock vs time for various gridblock sizes.

injection well reads:

$$Q_T = Q_g + Q_w$$

$$= kA [FM \cdot \lambda_g(r_w) |\nabla P_g| + \lambda_w(r_w) |\nabla P_w|] \quad (10)$$

with Q , λ and ∇P respectively representing a flow rate, a mobility and a pressure gradient associated to a fluid phase; r_w , k and A are the well radius, the absolute permeability of the perforated layer and its cross-sectional area. Constraining flow rates is important since the apparent viscosity of foam is known to heavily depend on its quality $f_g = Q_g/Q_T$ [1, 39]. Therefore, considering a isotropic radial foam flow in a homogeneous reservoir where capillary pressure and gravity can be neglected, pressure can be written as:

$$P(r) = P_f + \frac{Q_T}{2\pi h k \lambda_T(r_w)} \ln\left(\frac{r}{r_w}\right) \quad (11)$$

h being the perforation thickness, r the radial coordinate and $\lambda_T = \lambda_w + \lambda_g^f$ the total mobility. As previously performed

by van Poollen [30] in the case of fluids of constant viscosity, averaging this pressure over the well gridblock and identifying it with the well gridblock pressure yields:

$$P_0 \equiv \bar{P} = \frac{1}{2\pi h (r_0^2 - r_w^2)} \int_{r_w}^{r_0} 2\pi h r P(r) dr \quad (12)$$

which can be rearranged, after integration, as:

$$Q_T = \frac{2\pi h k \lambda_T(r_w)}{\ln\left(\frac{r_0}{r_w}\right) - \frac{1}{2}} (P_0 - P_f)$$

$$= WI_0 \cdot \lambda_T(r_w) (P_0 - P_f) \quad (13)$$

which is valid if terms varying in $(r_w/r_0)^2$ are negligible i.e. if $r_0 \gg r_w$.

If now we want to establish, for a given flow rate, a well index WI that integrates non-Newtonian effects for all well

A modified well index to account for shear-thinning behaviour in foam EOR simulation

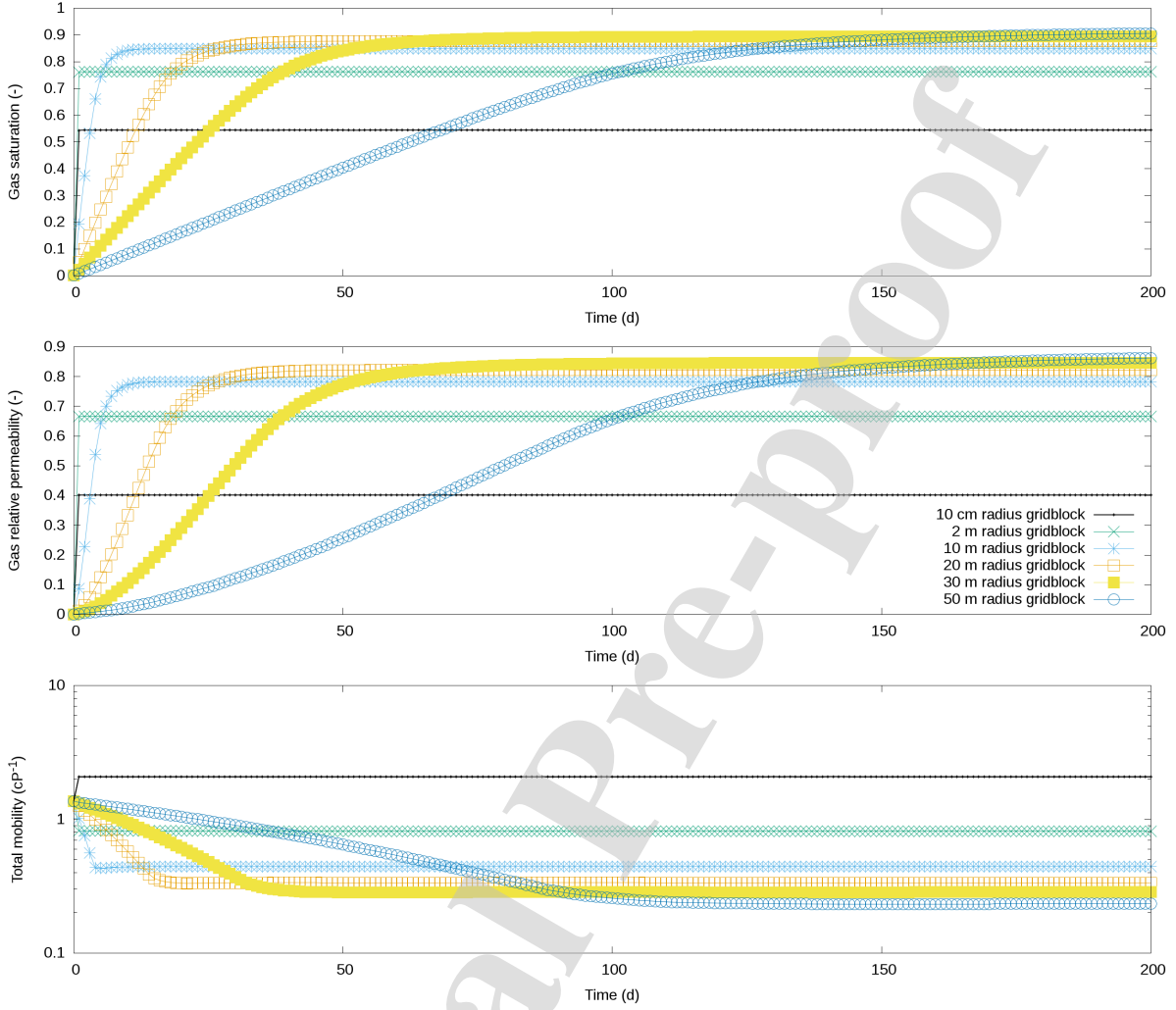


Figure 8: Radial model – gas saturation, gas relative permeability and total fluid mobility in well gridblock vs time for various gridblock sizes.

271 gridblock radius r_0 , we shall write in a general manner:

$$Q_T \equiv WI \cdot \overline{\lambda_T} (P_0 - P_f) \quad (14)$$

272 $\overline{\lambda_T}$ being the averaged total mobility over the well gridblock
 273 (yet to be determined). Equating the right hand sides of the
 274 two well flow rate / pressure relationships Eqs (13) and (14)
 275 yields a modified well index WI that can be computed from
 276 the conventional Peaceman well index WI_0 and the averaged
 277 total mobility $\overline{\lambda_T}$ over the well gridblock in the following
 278 manner:

$$WI = WI_0 \cdot \frac{\lambda_T(r_w)}{\overline{\lambda_T}} \quad (15)$$

279 In the case of foam obtained by co-injection, the total mo-
 280 bility reads $\lambda_T = \lambda_w + FM \cdot \lambda_g$. We may therefore write:

$$\begin{aligned} WI &= WI_0 \cdot \frac{\lambda_w(r_w) + FM(r_w) \cdot \lambda_g(r_w)}{\overline{\lambda_w + FM \cdot \lambda_g}} \\ &= WI_0 \cdot \frac{\lambda_w(r_w)}{\overline{\lambda_w}} \frac{1 + FM(r_w) \cdot \frac{\lambda_g(r_w)}{\lambda_w(r_w)}}{1 + \frac{FM \cdot \overline{\lambda_g}}{\overline{\lambda_w}}} \end{aligned} \quad (16)$$

282 This modified well index includes effects of saturation, 282
 283 shear-thinning rheology and gridblock dimension through 283
 284 the well gridblock averaged mobilities and FM . However, 284
 285 it demands an evaluation of several averages of complex sat- 285
 286 uration functions depending on both space and time. These 286
 287 could, assuming steady-state, be estimated using fractional 287
 288 flow theory (including shear-thinning effects such as in Zhou 288
 289 et al. [43] and Namdar et al. [40] for example). This is the 289
 290 subject of ongoing work. 290

A modified well index to account for shear-thinning behaviour in foam EOR simulation

At the well, foam quality f_g is controlled and constant. We may therefore write:

$$f_g = \frac{Q_g}{Q_T} = \frac{FM(r_w) \cdot \lambda_g(r_w)}{\lambda_w(r_w) + FM(r_w) \cdot \lambda_g(r_w)} \quad (17)$$

which results in:

$$FM(r_w) \cdot \frac{\lambda_g(r_w)}{\lambda_w(r_w)} = \frac{f_g}{1 - f_g} \quad (18)$$

This reformulates Eq. (16) as:

$$WI = WI_0 \cdot \frac{\lambda_w(r_w)}{\lambda_w} \frac{1 + \frac{f_g}{1 - f_g}}{1 + \frac{FM \cdot \lambda_g}{\lambda_w}} \quad (19)$$

Here, we choose to further simplify Eq. (19) by assuming the following:

- Saturation effects in the displacement are neglected, i.e. we assume that $\overline{\lambda_w} \approx \lambda_w(r_w)$. This assumption is obviously not satisfied for transient states. In the following, we show that this approximation is acceptable at steady-state.
- At steady-state, if one considers a coarse well gridblock whose radius r_0 is much larger than the well radius, one can infer that foam is going to be overall very efficient and develop a large mobility reduction over the well gridblock. In such a limiting case, one may have $FM \cdot \lambda_g / \lambda_w \approx 0$ as long as the foam maximum mobility reduction M_{ref} is large enough to dominate the mobility ratio λ_g / λ_w , roughly speaking. For instance, if the considered foam is such that $M_{ref} \sim 10,000$ while $\lambda_g / \lambda_w \sim 100 - 1,000$, this approximation should hold since $\overline{FM \cdot \lambda_g / \lambda_w} \sim (\lambda_g / \lambda_w) / M_{ref} \sim 0.01 - 0.1$.

With these assumptions we may write:

$$WI \approx WI_0 \cdot \left(1 + \frac{f_g}{1 - f_g}\right) \quad (20)$$

This is a heavily simplified expression compared to Eq. (16) that at first sight does not convey effects such as gridblock size or foam rheology. However, this expression of the well index, although perhaps flawed in its assumptions, is also much more practical to implement in a reservoir simulator through simple well index multipliers. We show in the following section that it manages to accurately capture shear-thinning behaviour in spite of its simplified nature.

5. Validation of the simplified well index

5.1. Radial gridding

5.1.1. Gas-water system

The simplified version of the modified well index is first validated in the initially water-saturated two-phase system

described above. Since the injector well is operating on rate constraints for each co-injected phase, foam quality is controlled and known: $f_g = 0.8$. Eq. (20) becomes $WI = 5 \times WI_0$. As shown in Fig. 9, for a gridblock radius of 50 m, there is a strong overestimation of bottom hole pressure compared to the reference case when the Peaceman well index is used. The modified well index on the other hand gives a better prediction of bottom hole pressure at the steady-state, with an error of 8 bar on the reference compared to 72 bar with the Peaceman formula. The large discrepancy observed before 120 days is due to saturation effects as the transient regime still dominates the displacement.

Fig. 10 summarizes the results obtained at steady-state for various gridblock sizes. The results show that while the Peaceman well index gives erroneous calculations of well bottom hole pressures, the modified well index gives a more realistic evaluation, even for large well gridblocks; a 100 m radius well gridblock underestimates the steady-state bottom hole pressure by 17 bar with the modified well index while the Peaceman formula overestimates it by 105 bar.

We now consider a modified initial state, with gas present at a saturation of 50%, all other parameters remaining unchanged. Apart from the duration of the transient state it does not significantly alters the pressure profile as seen in Fig. 11: the modified well index matches the reference result satisfyingly (with an error of 6 bar at 200 days) whereas the Peaceman formula results in an overestimation by 75 bar of the bottom hole pressure.

5.1.2. Three-phase system

An oil phase is introduced here; its viscosity is equal to 1.16 cP and its residual saturation to both water and gas is assumed to be zero (relative permeability curves are reproduced in Fig. 12). The dependency of foam to oil saturation is still neglected. We consider two initial states: one close to a typical tertiary recovery state where there is 80% of water and 20% of oil, and a second case where the reservoir is initially saturated in oil. The first case shows little difference with the two-phase system; the bottom hole pressures (BHP) observed at steady-state are slightly greater (reference grid: 273 bar; 50 m radius well gridblock grid, Peaceman well index: 361 bar; 50 m radius well gridblock grid, modified well index: 258 bar). Overall the variations of the discrepancy of steady-state BHP between the coarse grids and the reference grid observed in Figs 13 and 14 are similar to those observed in Figs 9 and 10.

The second case displays strongly degraded injectivities on the coarsest grids; the BHP obtained with the Peaceman calculation on a 50 m gridblock radius reaches 575 bar within 40 days of injection (Fig. 15). A 100 m gridblock radius overestimates the bottom hole pressure at steady-state by 262 bar when the Peaceman formula is used, which is a significant discrepancy. Applying the modified well index reduces this error to 63 bar, a more acceptable result (Fig. 16).

In both cases, the modified well index we propose manages to reduce the error on injectivity due to coarse gridding in a significant way. In the next section we will show that it

A modified well index to account for shear-thinning behaviour in foam EOR simulation

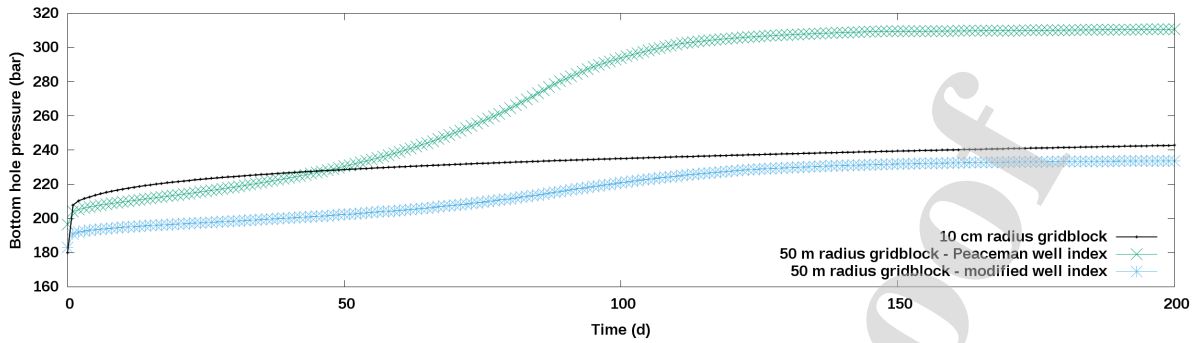


Figure 9: Radial model – injector bottom hole pressure vs time for a gridblock size $r_0 = 50$ m, obtained with the conventional Peaceman formula and the modified well index.

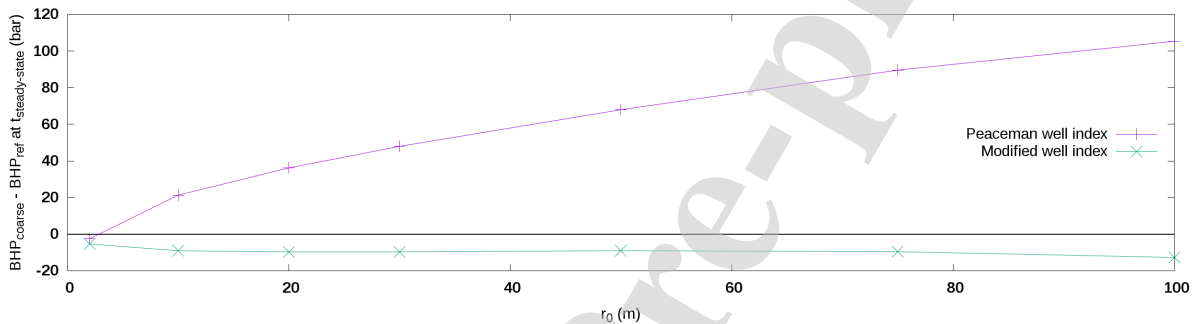


Figure 10: Radial model – injector bottom hole pressure at steady-state vs gridblock size, obtained with the conventional Peaceman formula and the modified well index.

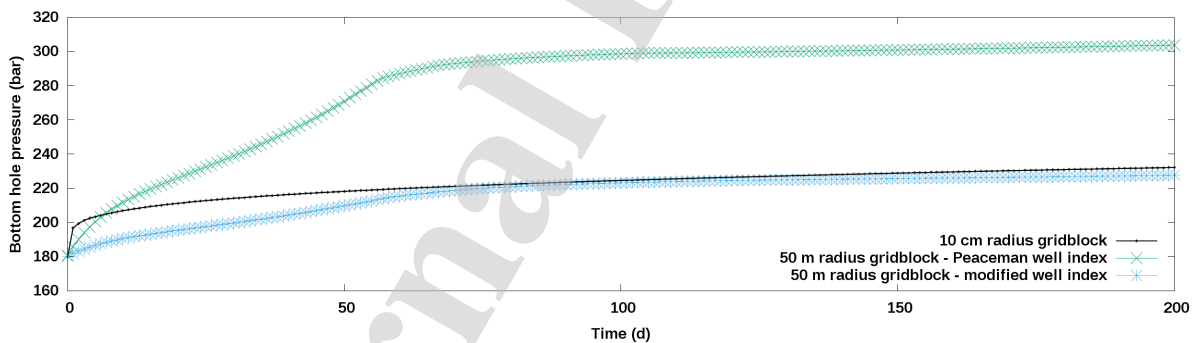


Figure 11: Radial model – initial water saturation of 50% – injector bottom hole pressure vs time for a gridblock size $r_0 = 50$ m, obtained with the conventional Peaceman formula and the modified well index.

384 also yields satisfying results on cartesian grids.

385 5.2. Cartesian gridding

386 We reproduce a similar analysis on Cartesian grids. As
 387 previously a reference case on a fine resolution mesh is created,
 388 with a 0.5×0.5 m well gridblock, this time using multiple
 389 grid refinements as shown in Fig. 17. Fig. 18 compares the two
 390 reference, fine scale models between radial and Cartesian geometries;
 391 the bottom hole pressures obtained are in close agreement.

392 As previously we compare the injector bottom hole pressures
 393 obtained with the conventional Peaceman approach and
 394

our proposed well index. Results are displayed in Fig. 19 for
 395 a 50×50 m well gridblock. Although it is still overestimated
 396 with the modified formula, the bottom hole pressure is closer to
 397 the reference and the error on injectivity is considerably reduced,
 398 from a 250 bar overpressure to 50 bar. Fig. 20 summarizes the
 399 evolution of the error in BHP related to well gridblock size;
 400 although it stays within a 50 bar error for a well gridblock radii
 401 smaller than 30 m, coarser well gridblocks used with the Peaceman
 402 formula yields overestimations of the BHP ranging from 175 bar to
 403 300 bar which is considerable. The modified well index manages to
 404 render smaller errors even for gridblock radii up to 100 m. It is no
 405
 406

A modified well index to account for shear-thinning behaviour in foam EOR simulation

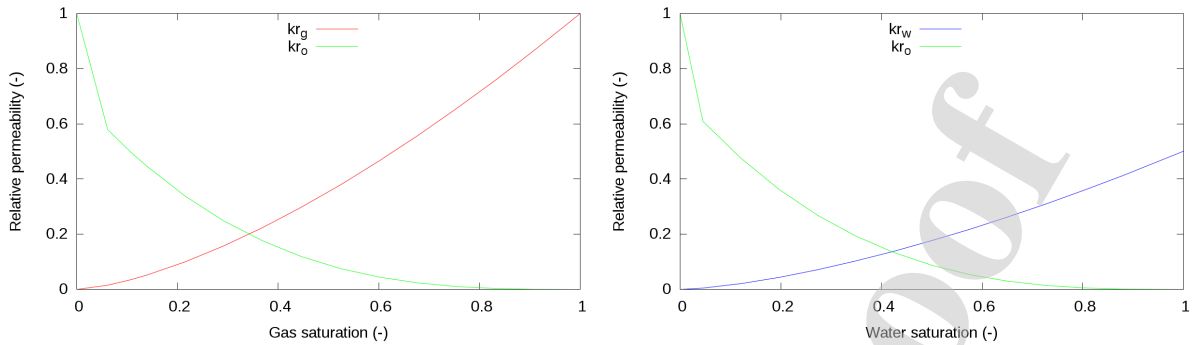
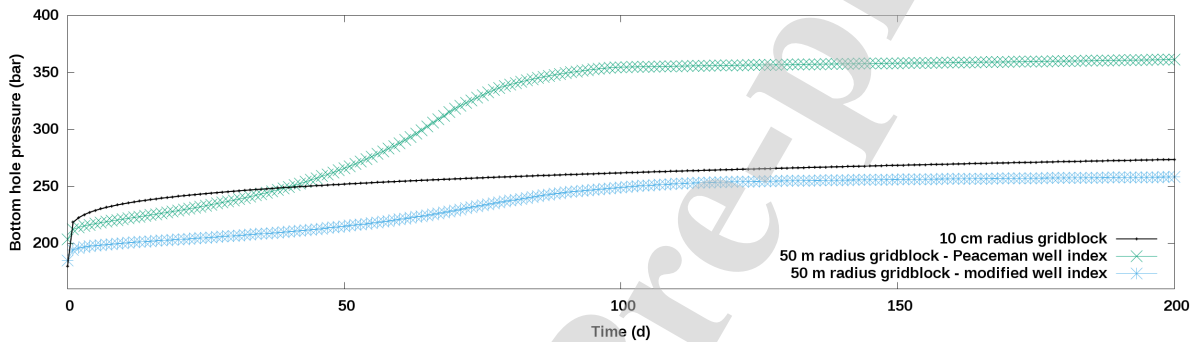


Figure 12: Relative permeability curves used in the three-phase system.

Figure 13: Radial model – initial oil saturation of 20% – injector bottom hole pressure vs time for a gridblock size $r_0 = 50$ m, obtained with the conventional Peaceman formula and the modified well index.

407 table that, compared to its application on radial grids where
 408 it overestimated injectivity, the modified well index under-
 409 estimates injectivity when used with cartesian grids. At this
 410 stage the authors of this paper are not certain why this hap-
 411 pens; an explanation could be the difference in the pressure
 412 gradient calculation between radial and cartesian geometries
 413 as cartesian grids do not capture near wellbore flow as accu-
 414 rately as radial grids especially with coarse spatial resolu-
 415 tions.

416 If the presence of oil is considered, it further increases
 417 the error obtained with the Peaceman formula, whereas the

418 estimate obtained with the modified well index remains closer
 419 to the reference bottom hole pressure (Figs 21 and 22). How-
 420 ever, since pressure is heavily dependent on the relative per-
 421 meability curves this cannot be generalized to any case.

6. Discussion

422 Although in the considered cases our modified well index
 423 gives an overall fairer prediction of injectivity than the
 424 Peaceman formula, it can still be improved. Indeed, in this
 425 work we only validated a simplified expression of the modi-
 426 fied well index. Neglecting saturation effects can be accept-
 427

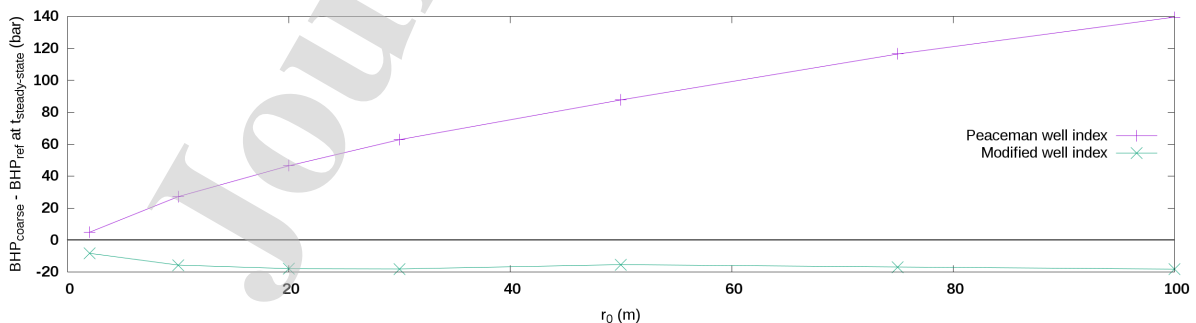


Figure 14: Radial model – initial oil saturation of 20% – injector bottom hole pressure at steady-state vs gridblock size, obtained with the conventional Peaceman formula and the modified well index.

A modified well index to account for shear-thinning behaviour in foam EOR simulation

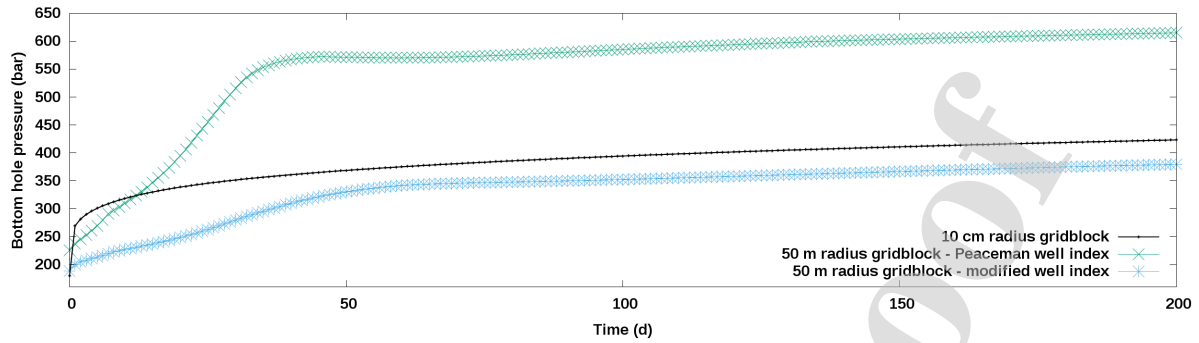


Figure 15: Radial model – initial oil saturation of 100% – injector bottom hole pressure vs time for a gridblock size $r_0 = 50$ m, obtained with the conventional Peaceman formula and the modified well index.

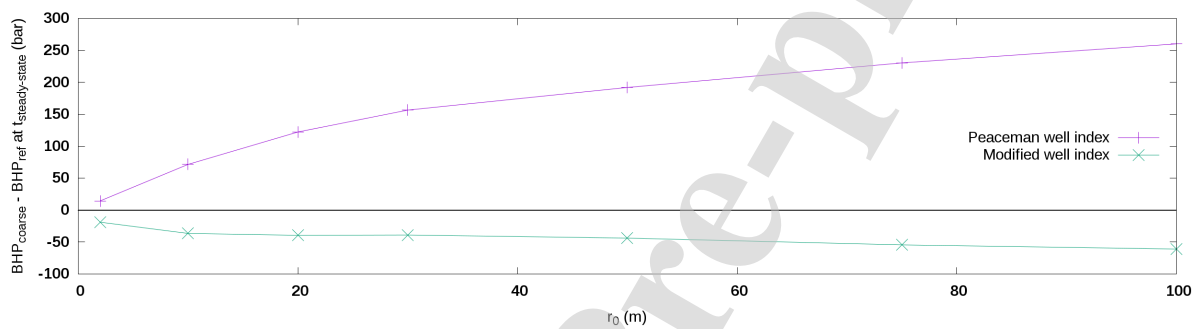


Figure 16: Radial model – initial oil saturation of 100% – injector bottom hole pressure at steady-state vs gridblock size, obtained with the conventional Peaceman formula and the modified well index.

428 able at steady-state, however if one wishes to be predictive
 429 even at the early stage of the injection they should be
 430 accounted for. In order to do so the terms we chose to ap-
 431 proximate would need to be evaluated. An approach using
 432 fractional flow theory could be considered as a framework
 433 to obtain the averages of the saturation dependent functions

434 that we approximated. A further stage would consist in de-
 435 riving a well index model including the mobility of oil.

436 Moreover, one may wonder whether a foam quality-based
 437 well index is a good idea, given that in field conditions qual-
 438 ity can hardly be controlled. However it is the main criteria
 439 used to describe foam flow during laboratory experiments

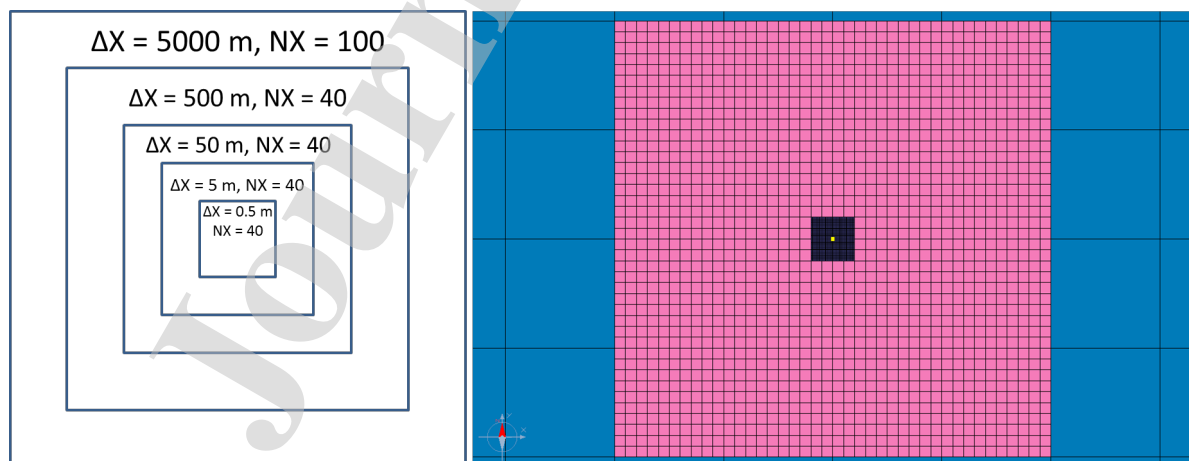


Figure 17: Cartesian model – sketch showing the repeated grid refinements used to build a reference, fine resolution mesh (left) top-down view of the reference grid (right).

A modified well index to account for shear-thinning behaviour in foam EOR simulation

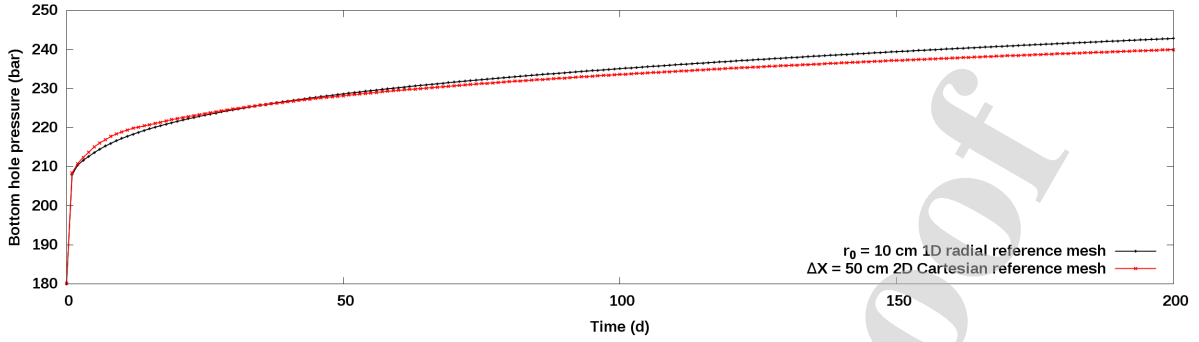


Figure 18: Cartesian model – bottom hole pressure of the injector well for a $\Delta x = 50$ cm case, compared with $r_0 = 10$ cm radial grid.

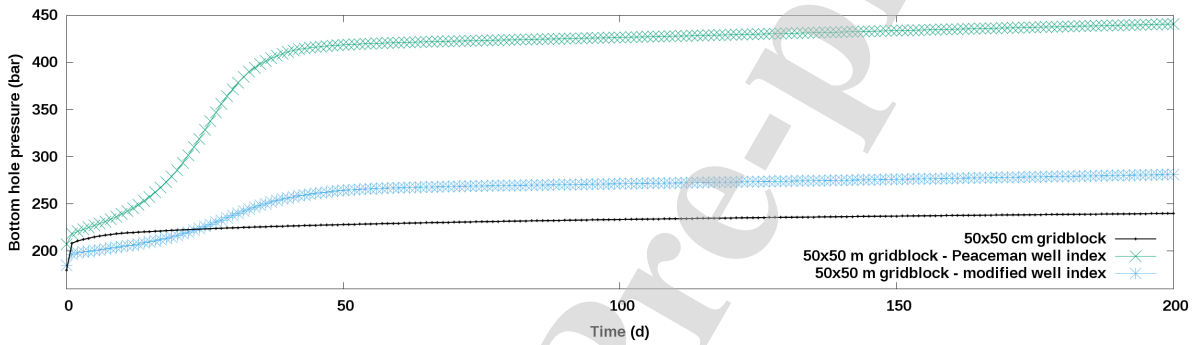


Figure 19: Cartesian model – initial water saturation of 100% – injector bottom hole pressure vs time for a gridblock size $\Delta x_0 = 50$ m, obtained with the conventional Peaceman formula and the modified well index.

440 and is included in most models; therefore it has to be reck- 451
 441 oned with. 452

442 Additionally, phenomena such as foam dry-out and oil 453
 443 saturation would need to be studied as they can have a con- 454
 444 siderable impact on foam stability. We studied rate con- 455
 445 strained injector wells and continuous surfactant injections; 456
 446 it would seem appropriate to validate the model on other 457
 447 configurations as well such as pressure constrained wells or 458
 448 surfactant slugs injections. Although we did not consider 459
 449 the effect of poorly captured injectivity away from the well 460
 450 gridblock, it can be expected to impact issues commonly en- 461

countered in reservoir simulation such as fingering. A field 451
 scale simulation would need to take such phenomena into 452
 account. 453

Ideally, the proposed correction should also address the 454
 transient state; approaches such as Archer's [3, 2] could be 455
 considered. 456

We demonstrated that it was possible, using a modified 457
 well index formula, to accurately capture shear-thinning be- 458
 haviour in foam injections; however, another approach, con- 459
 sisting in numerically matching coarse grids results on a re- 460
 ference grid by adjusting the well index could be considered. 461

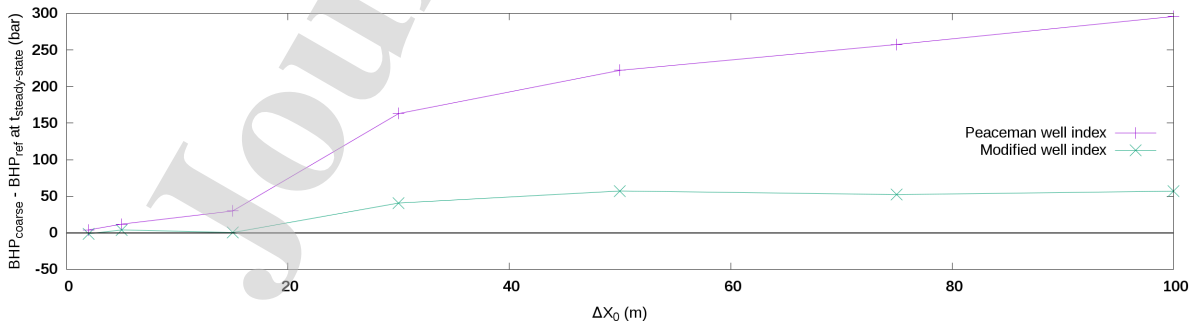


Figure 20: Cartesian model – initial water saturation of 100% – injector bottom hole pressure at steady-state vs gridblock size, obtained with the conventional Peaceman formula and the modified well index.

A modified well index to account for shear-thinning behaviour in foam EOR simulation

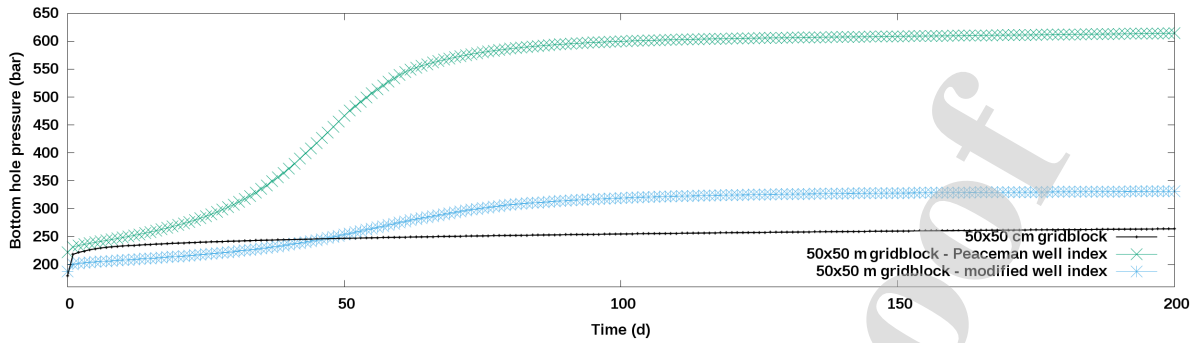


Figure 21: Cartesian model – initial oil saturation of 20% – injector bottom hole pressure vs time for a gridblock size $\Delta x_0 = 50$ m, obtained with the conventional Peaceman formula and the modified well index.

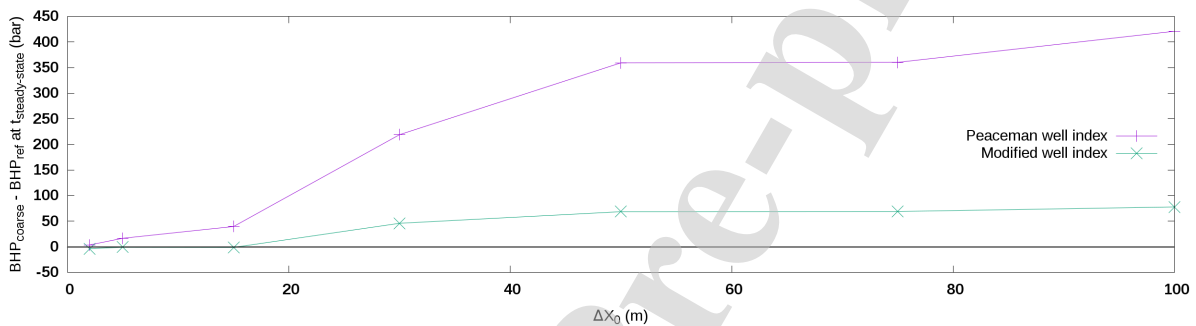


Figure 22: Cartesian model – initial oil saturation of 20% – injector bottom hole pressure at steady-state vs gridblock size, obtained with the conventional Peaceman formula and the modified well index

462 For large, multiple wells field cases, single well models could
 463 be built to achieve this within reasonable computational costs;
 464 an example of such a methodology is sketched in Fig. 23.
 465 The simplified, quality-based expression of the well index
 466 given in Eq. (20) could be used as an initial value in the
 467 matching process. This approach corrects all the biases in
 468 the well behaviour due to gridding; saturation, composition
 469 and velocity gradients are accounted for. The validation of
 470 this sort of workflow is the subject of ongoing work.

471 7. Summary and conclusions

472 The following conclusions can be drawn:

- 473 • It was shown that the simulation of foam injection estimates
 474 drastic overpressures at the wellbore when the
 475 conventional Peaceman formula is used to calculate
 476 well injectivity in reservoir simulators. This is due to
 477 an underestimation of the foam velocity in the well
 478 gridblock and to saturation and dilution effects. Poor
 479 injectivity ensues and degraded economics are to be
 480 expected.
- 481 • A modified well index was developed to include shear-
 482 thinning effects in foam injectivity calculations in reser-
 483 voir simulators. Its full form takes into account the
 484 effects of foam rheology and grid size as well as satu-

485 ration effects in the transient regime. It may be calcu-
 486 lated using fractional flow theory.

- 487 • In the scope of this paper a simplified expression of
 488 this modified well index was derived, based mostly
 489 on the quality of the foam. The implementation of
 490 this simplified expression is straightforward and can
 491 be used in any simulator in which semi-empirical foam
 492 models are used. It was first validated by comparing
 493 simulation results on two-phase radial 1D systems of
 494 different gridblock sizes and initial saturation states.
 495 The results obtained with the modified well index were
 496 satisfying in all considered cases as it considerably re-
 497 duced the error on foam injectivity in coarser grids
 498 compared to the Peaceman formula.
- 499 • First steps towards reservoir model validation were made
 500 as the simplified expression was validated on three-
 501 phase systems as well as on Cartesian grids. Further
 502 work would include petrophysical heterogeneity as well
 503 as 3D simulation in order to further validate the well
 504 index on pilot or field scale models.

CRediT authorship contribution statement

505 **A. Soulat:** Investigation, Conceptualization, Methodol-
 506 ogy, Formal analysis, Data curation, Resources, Visualiza-
 507 tion, Writing - Original Draft, Writing - Review & Editing.
 508

A modified well index to account for shear-thinning behaviour in foam EOR simulation

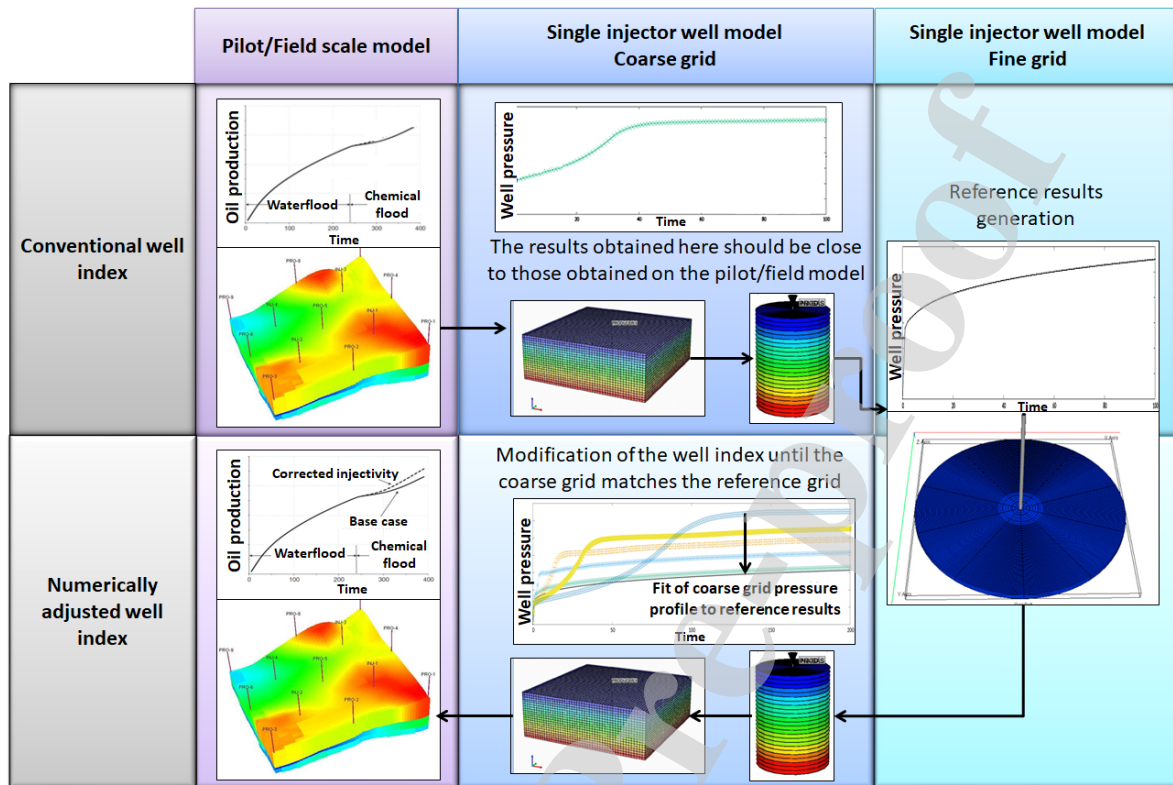


Figure 23: Sketch describing a numerical adjustment based modification of the well index (contains subfigures adapted from [22]).

509 **F. Douarche:** Investigation, Conceptualization, Methodology, Formal analysis, Writing - Review & Editing, Supervision. **E. Flauraud:** Data curation, Software, Resources.

512 References

- 513 [1] Alvarez, J.M., Rivas, H., Rossen, W.R., 2001. A unified model for
514 steady-state foam behavior at high and low foam qualities. SPE Journal
515 6, 325–333. Paper SPE 74141.
- 516 [2] Archer, R., 2010. Transient well indices: A link between analytical
517 solution accuracy and coarse grid efficiency. Paper SPE 134832 presented
518 at the SPE Annual Technical Conference and Exhibition held in Florence,
519 Italy, 19-22 September.
- 520 [3] Archer, R., Yildiz, T., 2001. Transient well indices for numerical
521 well test analysis. Paper SPE 71572 presented at the SPE Annual
522 Technical Conference and Exhibition held in New Orleans, Louisiana,
523 30 September - 3 October.
- 524 [4] Batôt, G., Fleury, M., Nabzar, L., 2016. Study of CO₂ foam performance
525 in a CCS context. Paper presented at the 30th International
526 Symposium of the Society of Core Analysts, Snowmass, Colorado,
527 USA, 21-26 August 2016.
- 528 [5] Beunat, V., Batôt, G., Gland, N., Chevallier, E., Cuenca, A., 2019. Influence
529 of wettability and oil saturation on the rheological behavior of
530 CO₂-foams. Paper presented at the EAGE 20th European Symposium
531 on Improved Oil Recovery, Pau, France, 8-11 April 2019.
- 532 [6] Boeije, C.S., Rossen, W.R., 2015. Fitting foam-simulation-model
533 parameters to data: I. Coinjection of gas and liquid. SPE Reserv. Eval.
534 Eng. 18, 264–272.
- 535 [7] Braconnier, B., Flauraud, E., Nguyen, Q.L., 2014. Efficient scheme

for chemical flooding simulation. Oil & Gas Science and Technology
– Rev. IFP Energies nouvelles 69, 585–601.

- 536 [8] Coats, K., George, W., Chu, C., Marcum, B., 1974. Three-
537 dimensional simulation of steam-flooding. SPE Journal 257, 573–
538 592.
- 539 [9] Computer Modeling Group, 2015. STARS user's guide, version 2015.
540 Calgary, Alberta, Canada.
- 541 [10] Falls, A., Musters, J.J., Ratulowski, J., 1989. The apparent viscosity
542 of foams in homogeneous bead packs. SPE Reserv. Eng. 4, 155–164.
- 543 [11] Gassara, O., Douarche, F., Braconnier, B., Bourbiaux, B., 2017. Equivalence
544 between semi-empirical and population-balance foam models. Transport
545 in Porous Media 120, 473–493.
- 546 [12] Gassara, O., Douarche, F., Braconnier, B., Bourbiaux, B., 2020. Calibrating
547 and scaling semi-empirical foam flow models for the assessment of
548 foam-based EOR processes (in heterogeneous reservoirs). Transport
549 in Porous Media 131, 193–221.
- 550 [13] de Gennes, P.G., Brochard-Wyart, F., Quéré, D., 2004. Capillarity and
551 wetting phenomena: drops, bubbles, pearls, waves. Springer-Verlag.
- 552 [14] Gong, J., Vincent-Bonnieu, S., Bahrim, R.Z.K., 2018. Modelling of
553 liquid injectivity in surfactant-alternating-gas foam enhanced oil
554 recovery. Paper SPE 190435 presented at the SPE EOR Conference at
555 Oil and Gas West Asia, Muscat, Oman, 26-28 March 2018.
- 556 [15] Hirasaki, G.J., Lawson, J.B., 1985. Mechanisms of foam flow in
557 porous media: apparent viscosity in smooth capillaries. SPE Journal
558 25. Paper SPE 12129.
- 559 [16] IFP Energies nouvelles, 2018. PumaFlow 10.0 reference manual.
560 France.
- 561 [17] Kaminsky, R.D., Wattenbargern, R.C., Szafranski, R.C., 2007. Guidelines
562 for polymer flooding evaluation and development. Paper IPTC 11200
563 presented at IPTC 2007: International Petroleum tech-
564 565

A modified well index to account for shear-thinning behaviour in foam EOR simulation

- 566 nology Conference, Dubai, UAE, 4-6 December 2007.
- 567 [18] Kuehne, D.L., Ehman, D.I., Emanuel, A.S., Magnani, C.F., 1990. De- 634
568 sign and evaluation of a nitrogen-foam field trial. *J. Petr. Technol.* 42, 635
569 504–512. 636
- 570 [19] Kumar, V., Pal, N., Jangir, A.K., Manyala, D.L., Varade, D., Mandal, 637
571 A., Kuperkar, K., 2020. Dynamic interfacial properties and tuning 638
572 aqueous foamability stabilized by cationic surfactants in terms of their 639
573 structural hydrophobicity, free drainage and bubble extent. *Colloids 640
574 and Surfaces A* 588. 641
- 575 [20] Lake, L.W., 1989. *Enhanced oil recovery*. Prentice Hall, Englewood 642
576 Cliffs, New Jersey, USA. 643
- 577 [21] Leeftink, T., Latooj, C., Rossen, W., 2015. Injectivity errors in simu- 644
578 lation of foam EOR. *Journal of Petroleum Science and Engineering* 645
579 126, 26–34. 646
- 580 [22] Li, Z., Delshad, M., 2014. Development of an analytical injectivity 647
581 model for non-Newtonian polymer solutions. *SPE Journal* 19, 381– 648
582 389. Paper SPE 163672. 649
- 583 [23] Li, Z., Fortenberry, R., Luo, H., Delshad, M., 2017. An examina- 650
584 tion of the concept of apparent skin factor in modeling injectivity of 651
585 non-Newtonian polymer solutions. *Journal of Petroleum Science and 652
586 Engineering* 158, 160–174. 653
- 587 [24] Lotfollahi, M., Farajzadeh, R., Delshad, M., Varavei, A., Rossen, W., 654
588 2016. Comparison of implicit-texture and population-balance foam 655
589 models. *Journal of Natural Gas Science and Engineering* 31, 184– 656
590 197. 657
- 591 [25] Ma, K., Farajzadeh, R., Lopez-Salinas, J.L., Miller, C.A., Biswal, 658
592 S.L., Hirasaki, G.J., 2014a. Non-uniqueness, numerical artifacts, and 659
593 parameter sensitivity in simulating steady-state and transient foam 660
594 flow through porous media. *Transport in Porous Media* 102, 325– 661
595 348. 662
- 596 [26] Ma, K., Ren, G., Mateen, K., Morel, D., Cordelier, P., 2014b. Lit- 663
597 erature review of modeling techniques for foam flow through porous 664
598 media. Paper SPE 169104 presented at the SPE Improved Oil Recov- 665
599 ery Symposium held in Tulsa, Oklahoma, USA, 12-16 April 2014. 666
- 600 [27] Martinsen, H.A., Vassenden, F., 1999. Foam-assisted water alternat- 667
601 ing gas (FAWAG) process on Snorre. Paper presented at the 1999 668
602 European IOR Symposium, Brighton, U.K., 18-20 August 1999. 669
- 603 [28] Peaceman, D., 1978. Interpretation of well-block pressures in numer- 670
604 ical reservoir simulation. *SPE Journal* 18, 182–194. 671
- 605 [29] Peaceman, D., 1983. Interpretation of well-block pressures in numer- 672
606 ical reservoir simulation with nonsquare grid blocks and anisotropic 673
607 permeability. *SPE Journal* 23, 531–543. 674
- 608 [30] van Poolen, H., Bixel, H., Jargon, J., 1970. Individual well pressures 675
609 in reservoir modeling. *Oil and Gas Journal* , 78–80. 676
- 610 [31] van Poolen, H., Breitenbach, E., Thurnau, D., 1968. Treatment of 677
611 individual wells and grids in reservoir modeling. *SPE Journal* , 341– 678
612 346. 679
- 613 [32] Rossen, W.R., 1996. *Foams: Theory, measurements and applications*. 680
614 Marcel Dekker, New York. chapter *Foams in enhanced oil recovery*. 681
615 pp. 413–464. 682
- 616 [33] Rossen, W.R., van Duijn, C.J., Nguyen, Q.P., Shen, C., Vikingstad, 683
617 A.K., 2010. Injection strategies to overcome gravity segregation in 684
618 simultaneous gas and water injection into homogeneous reservoirs. 685
619 *SPE Journal* 15, 70–90. 686
- 620 [34] Schlumberger, 2010. *Eclipse reservoir simulation software, version 687
621 2010.2, technical description*. 688
- 622 [35] Schramm, L.L., 1994. *Foams: Fundamentals and applications in the 689
623 petroleum industry*. ACS Advances in Chemistry Series no 242, Am. 690
624 Chem. Soc., Washington, DC. 691
- 625 [36] Seright, R.S., Seheult, M., Talashek, T., 2009. Injectivity characteris- 692
626 tics of EOR polymers. *SPE Journal* 12, 783–792. Paper SPE 115142. 693
- 627 [37] Sharma, A., Delshad, M., Huh, C., Pope, G.A., 2011. A practical 694
628 method to calculate polymer viscosity accurately in numerical reser- 695
629 voir simulator. Paper SPE 147239 presented at the SPE Annual Techn- 696
630 ical Conference and Exhibition held in Colorado, Denver, USA, 31 697
631 October - 2 November. 698
- 632 [38] Weaire, D., Hutzler, S., 1999. *The physics of foams*. Oxford Univer- 699
633 sity Press. 700
- [39] Xu, Q., Rossen, W.R., 2000. Dynamic viscosity of foam in porous media. Paper presented at the Proc. Euro. Conference on Foams, Emulsions and Applications, Delft, The Netherlands. 5-8 June, 2000. 634
635
636
- [40] Zanganeh, M.N., Kam, S.I., LaForce, T.C., 2011. The method of characteristics applied to oil displacement by foam. *SPE Journal* 16, 8–23. Paper SPE 121580. 637
638
639
- [41] Zanganeh, M.N., Rossen, W.R., 2013. Optimization of foam EOR: Balancing sweep and injectivity. *SPE Reservoir Evaluation and Engineering* 16. Paper SPE 163109. 640
641
642
- [42] Zeng, Y., Muthuswamy, A., Ma, K., Wang, L., Farajzadeh, R., Puerto, M., Vincent-Bonnieu, S., Eftekhari, A.A., Wang, Y., Da, C., Joyce, J.C., Biswal, S.L., Hirasaki, G.J., 2016. Insights on foam transport from a texture-implicit local-equilibrium model with an improved parameter estimation algorithm. *Ind. Eng. Chem. Res.* , 7819–7829. 643
644
645
646
647
- [43] Zhou, Z., Rossen, W.R., 1995. Applying fractional flow theory to foam processes at the limiting capillary pressure. *SPE Adv. Technol. Ser.* 3, 154–162. 648
649
650
651
652
653
654
655
656
657
658
659
660
661
662
663
664
665
666
667
668
669
670
671
672
673
674
675
676
677
678
679
680
681
682
683
684
685
686
687
688
689
690
691
692
693
694
695
696
697
698
699
700



Subject: Article submission highlights

Dear Editor,

Please find enclosed the highlights of our proposed article “A modified well index to account for shear-thinning behaviour in foam EOR simulation”:

- Most commercial simulators often overlook non-Newtonian behaviour due to inadequate grid resolution.
- Poor evaluation of near-wellbore velocity leads to erroneously degraded injectivity on coarser grids when compared to the sufficiently refined grids.
- New formulations of the well index that capture shear-thinning behaviour overlooked in the original Peaceman calculation are proposed.
- The accuracy of the calculated injectivity compared to the conventional Peaceman calculation is verified.

Best regards,

Antoine Soulat

Declaration of interests

The authors declare that they have no known competing financial interests or personal relationships that could have appeared to influence the work reported in this paper.

The authors declare the following financial interests/personal relationships which may be considered as potential competing interests:-

Journal Pre-proof



Subject: Article submission – Credit Authorship contribution statement

Dear Editor,

Please find enclosed the Credit Authorship contribution statement for our proposed article “A modified well index to account for shear-thinning behaviour in foam EOR simulation”:

- **Soulat:** Investigation, Conceptualization, Methodology, Formal analysis, Data curation, Resources, Visualization, Writing - Original Draft, Writing - Review & Editing.
- **F. Douarche:** Investigation, Conceptualization, Methodology, Formal analysis, Writing - Review & Editing, Supervision.
- **E. Flauraud:** Data curation, Software, Resources.

Best regards,

Antoine Soulat